Beyond Carbon *K*-Edge Harmonic Emission Using a Spatial and Temporal Synthesized Laser Field

J. A. Pérez-Hernández,[1,*] M. F. Ciappina,[2,3] M. Lewenstein,[2,4] L. Roso,[1] and A. Zaïr[5]

[1]*Centro de Láseres Pulsados (CLPU), Parque Científico, 37185 Villamayor, Salamanca, Spain*
[2]*ICFO-Institut de Ciènces Fotòniques, Mediterranean Technology Park, 08860 Castelldefels (Barcelona), Spain*
[3]*Department of Physics, Auburn University, Auburn, Alabama 36849, USA*
[4]*ICREA-Institució Catalana de Recerca i Estudis Avançats, Lluis Companys 23, 08010 Barcelona, Spain*
[5]*Department of Physics, Imperial College London, London SW7 2AZ, United Kingdom*

We present numerical simulations of high-order harmonic generation in helium using a temporally synthesized and spatially nonhomogeneous strong laser field. The combination of temporal and spatial laser field synthesis results in a dramatic cutoff extension far beyond the usual semiclassical limit. Our predictions are based on the convergence of three complementary approaches: resolution of the three dimensional time dependent Schrödinger equation, time-frequency analysis of the resulting dipole moment, and classical trajectory extraction. A laser field synthesized both spatially and temporally has been proven capable of generating coherent extreme ultraviolet photons beyond the carbon *K* edge, an energy region of high interest as it can be used to initiate inner-shell dynamics and study time-resolved intramolecular attosecond spectroscopy.

Near-edge x-ray absorption spectroscopy [1,2] is a very powerful technique for the probing of the local chemical environment of molecules. Combining to such a technique an attosecond time resolution will open a new route to explore ultrafast inner-shell charge dynamics in molecular systems. One example of this is the emergence of attosecond spectroscopy where the high harmonic generation process itself is used to probe ultrafast intracation dynamics in aligned molecules [3,4]. The high harmonic generation (HHG) process allowed a time-frequency mapping due to the attosecond chirp; therefore, the intracation dynamics is encoded in the harmonic spectra. It is therefore expected to be an important breakthrough in this field. One way to generate attosecond x-ray pulses is through the process of HHG driven by strong midinfrared laser fields as it is well known that the HHG cutoff scales as λ^2 (λ being the laser wavelength) [5]. A first experimental demonstration has been very recently done [6], but the high technological requirements on the midinfrared wavelength femtosecond laser source makes it very challenging. In addition, it has been demonstrated that the generation efficiency of the harmonic photons rapidly decreases with increasing laser wavelength according to a $\lambda^{-5.5}$ power law [7–9]. Hence, there is a high demand for alternative routes based on existing conventional femtosecond laser sources at 800 nm. So far a large number of strategies involving the tailoring of the input laser pulse for HHG have been implemented. Using a combination of fields of two or more colors to temporally synthesize the desired strong laser field [10–20], or using chirping techniques [21], seems like a promising route. The new approach we propose involves combining the two techniques to controllably shape the

final laser field both in time and in space. The temporal synthesis is performed using two few-cycle laser pulses delayed in time [22]. Few-cycle laser pulses are now commonly used for attoscience applications and are generated using a post-compression stage [23,24]. The spatial synthesis is obtained by using a nonhomogeneous laser field [25–27] produced, for instance, by nanoplasmonic antennas. The aim of this Letter is to demonstrate that performing field synthesis both in time and in space is a new route for the generation of photons at energies beyond the carbon *K* edge using 800 nm pulses, which can be obtained from conventional Ti:Sapph laser sources now relatively common among the strong field physics community.

To perform the temporal synthesis, we follow a method described in Ref. [22] where two 4-cycle pulses at 800 nm are delayed in time, as described by

$$E_1(t) = E_0 \sin^2\left(\frac{\omega t}{2N}\right)\sin(\omega t) \qquad (1)$$

$$E_2(t, \tau) = E_0 \sin^2\left(\frac{\omega(t - \tau)}{2N}\right)\sin(\omega(t - \tau) + \phi) \qquad (2)$$

where E_0 is the laser electric field amplitude in atomic units ($E_0 = \sqrt{I/I_0}$ with $I_0 = 3.5 \times 10^{16}$ W/cm²), $\omega = 0.057$ a.u. the laser frequency corresponding to $\lambda = 800$ nm, T the laser period, N the total number of cycles in the pulse, ϕ the carrier-envelope phase (CEP), and τ the time delay between the pulses. In our simulations we consider the case $N = 4$ and $\phi = 0$.

According to our numerical simulations, the optimal time delay between the two replica corresponds to $\tau = 1.29$ T. This way the resulting laser amplitude of the

synthesized field is equal to one of the two input pulse replica. The two replica have been taken with the same CEP because they are expected to be produced from the same initially CEP stabilized source and control on the CEP can be managed by using wedges. In such a configuration an extension of the cutoff has been predicted up to $4.5U_p$, where U_p is the quiver energy associated with the laser field ($U_p = \frac{I}{4\omega^2}$). Most of the numerical and semiclassical approaches used to study HHG in atoms and molecules consider a temporally and spatially homogeneous laser field [28,29]. Studies have been carried out on the effect of synthesized spatial profiles on pulses with homogeneous temporal distributions. For instance, in Ref. [30], a flat-top spatial profile beam was proposed for the production of isolated attosecond pulses, demonstrating that the control of the laser field in the spatial domain provides another way to control the HHG process.

Our idea is therefore to use not only a temporal synthesis, as provided by two CEP stabilized few-cycle pulses as described by Eqs. (1) and (2) (referred to as double-pulse configuration), but also a spatial synthesis (referred to as nonhomogeneous configuration). This nonhomogeneous spatial distribution of the laser field can be obtained experimentally by using a laser field as produced by nano-plasmonic antennas [25–27,31], metallic waveguides [32], metal [33,34] and dielectric nanoparticles [35], or metal nanotips [36–40]. The laser electric field is then no longer homogeneous in the region where the electron dynamics take place. Very recently, studies about how HHG spectra are modified due to nonhomogeneous fields, such as those present in the vicinity of a nanostructure irradiated by a short laser pulse, have been published [25–27,41], leading to the so called "plasmonic enhanced intensity" showing the growing interests such new fields.

In order to calculate the harmonic spectra we solve the three dimensional time dependent Schrödinger equation (3D-TDSE) in the length gauge while employing a double-pulse, nonhomogeneous driving laser field. The harmonic yield from a single atom is proportional to the Fourier transform of the dipole acceleration of its active electron and can be calculated from the time propagated electronic wave function. We have used our code, which is based on an expansion of spherical harmonics, Y_l^m, considering only the $m = 0$ terms due to the cylindrical symmetry of the problem. The numerical technique is based on a Crank-Nicolson method implemented on a splitting of the time-evolution operator that preserves the norm of the wave function. We base our studies in helium because a majority of experiments in HHG are carried out in noble gases. Hence we have considered in our 3D-TDSE code the atomic potential reported in Ref. [42] to describe accurately the helium atom. We remark that our scheme can be applied to any atom or molecule, once the adequate potential has been chosen. The coupling between the atom and the laser pulse, linearly polarized along the z axis, is

modified in order to treat the spatially nonhomogeneous fields as follows:

$$V_l(z, t, \tau) = \tilde{E}(z, t, \tau)z \qquad (3)$$

with

$$\tilde{E}(z, t, \tau) = E(t, \tau)(1 + \beta z) \qquad (4)$$

where V_l represents the laser-atom interaction in the length gauge, $E(t, \tau)$ is the laser field defined by the sum of the pulses described in Eqs. (1) and (2), the parameter β defines the strength of the nonhomogeneity, and the dipole approximation is preserved because $\beta \ll 1$.

The linear functional form for the spatial nonhomogeneity in Eq. (4) could be obtained engineering adequately the geometry of plasmonic nanostructures and by adjusting the laser parameters in such a way that the laser-ionized electron feels only a linear spatial variation of the laser electric field when in the continuum (see, e.g., Ref. [41] and references therein). The harmonic spectrum then obtained in helium for $\beta = 0.002$ is presented in Fig. 1. We can observe a considerable cutoff extension up to $12.5U_p$, which is much greater than when the double-pulse configuration is employed alone (it leads to a maximum of $4.5U_p$ [22]). This large extension of the cutoff is therefore a signature of the combined effect of the double pulse and the spatially nonhomogeneous character of the laser electric field. For this particular value of the laser peak intensity (1.4×10^{15} W/cm^2) the highest photon energy is greater than 1 keV. Note that the quoted intensity is actually the plasmonic enhanced intensity, not the input laser intensity. The latter could be several orders of magnitude smaller, according to the plasmonic enhancement factor (see, e.g., Refs. [31,32]) and will allow the nano-plasmonic target to survive to the interaction experimentally. Besides, under such interaction conditions, the field enhancement for the HHG occurs upon an interaction length in the range of 1 μm or less, so that no phase-matching condition consideration is required [32,43].

In addition to the case presented here ($N = 4$, CEP $= 0$), we have performed a systematic study upon the pulse duration N and the CEP value for different values of the β parameter. The optimum values were found to be
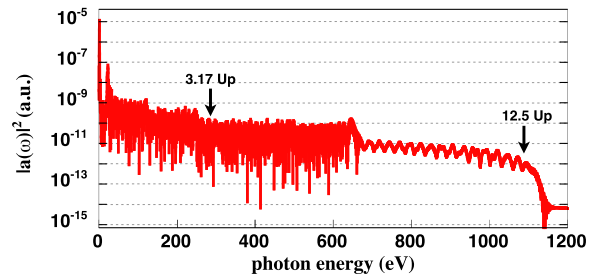
FIG. 1 (color online).   3D-TDSE harmonic spectrum in a helium atom generated by laser pulses described in Eq. (4) and $\beta = 0.002$ for a plasmonic enhanced intensity $I = 1.4 \times 10^{15}$ W/cm^2.

CEP $= 0$ and $N < 4$, corresponding to a maximum cutoff extension for each specific value of β and N.

In order to understand the mechanism linked to this particular extension of the cutoff, we investigated the classically retrieved trajectories by solving Newton's equation of motion for an electron in the laser field described in Eq. (4). We calculated the energy of the returning electron as a function of the time duration of the laser pulse [27]. A decrease in the harmonic yield is, however, observed beyond 650 eV in Fig. 1. This can be explained by the classical calculation presented in Fig. 2(d), where below 650 eV two trajectories contribute to the harmonic yield, inducing structures in the corresponding harmonic spectrum. Toward the cutoff energy, the excursion time of these trajectories increases, resulting in a harmonic yield drop due to the spreading of the electronic wave packet. Above 650 eV only one path survives, resulting in a continuum observed in the corresponding harmonic spectrum.

In Fig. 2 we show the classical rescattering energies (in eV) as a function of the ionization time, in blue (dark grey), and recombination times in black including the effect of the nonhomogeneous field varying the β parameter. The direct effect is that the amount of recombination event decreases as β increases. The spatial nonhomogeneity of the laser field strongly modified some of the high energetic trajectories. This modification forces these trajectories that do not recombine in the case of $\beta = 0$ to finally recombine when the inhomogeneity is present leading to a cutoff extension greater than 1 keV. Further to this selection and extension of photon energies, an additional very interesting effect linked to the nonhomogeneity of the laser field arises. Indeed, for the case of $\beta = 0.002$ the so-called "short" and "long" classical

trajectories [44–46] recombine now almost simultaneously. In other words, the nonhomogeneity of the laser field acts as a temporal lens that forces electrons ionized at different times to recombine around the same time, as shown in Fig. 2(d). This implies that the attosecond chirp is conserved for the short trajectory while it is strongly modified for the long trajectory.

In addition, the recollision time t_r of the electron is presented in Fig. 3 as a function of the ionization time t_i for several values of β. By considering ionization times between 1.25 and 2.25 optical cycles, the long trajectories are those with recollision times $t_r \gtrsim 2.5$ optical cycles. It is only for the case of homogeneous laser field, in grey (dark grey) lines in the figure, trajectories are clearly distinguishable. On the other hand, short trajectories are characterized by $t_r \lesssim 2.5$ optical cycles and these are present for both the homogeneous and nonhomogeneous cases. The results presented here are consistent with those shown in Refs. [26,27], except that in our case the laser pulse has a more complex temporal shape. This results from the fact that the long trajectories are modified both by the spatial nonhomogeneity and the temporal double-pulse configuration. As such the long trajectories in the homogeneous case ($\beta = 0$) with ionization times t_i around 1.25 and 1.75 optical cycles merge into unique trajectories. The trajectory with $t_i \sim 1.75$ now has its ionization times greater than half an optical cycle that get smaller while β increases. As a result, the time spent by the electron excursion in the continuum increases. The electric field strength at the ionization time for short trajectories being greater than for long trajectories, and considering that the ionization rate is a nonlinear function of this electric field, long trajectories are then less efficient than the short ones. On the other hand, short trajectories are almost
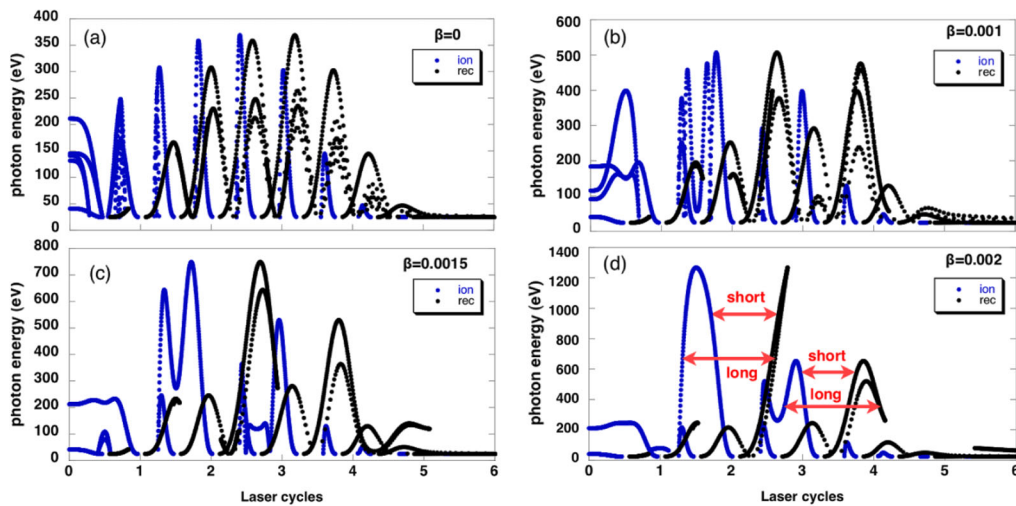
FIG. 2 (color online).   Rescattering energies of electrons as a function of the ionization time, in blue (dark grey), and recombination time in black, for laser pulses described in Eq. (4) for different values of $\beta = 0.0$ (a), $\beta = 0.001$ (b), $\beta = 0.0015$ (c) and $\beta = 0.002$ (d). In this case the plasmonic enhanced intensity is $I = 1.4 \times 10^{15}$ W/cm^2, which corresponds to the saturation intensity for He.
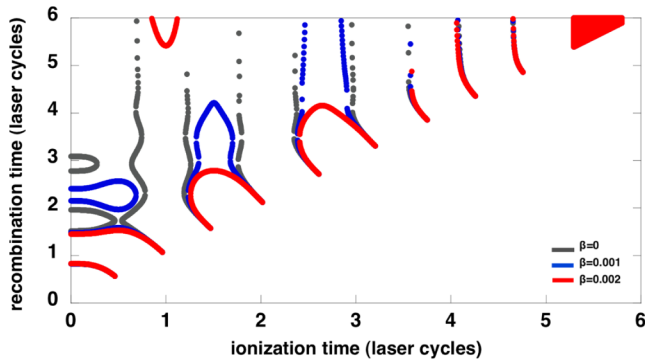
FIG. 3 (color online). Recombination times as a function of ionization times for three of the four cases shown in Fig. 2 for the He atom. The curve for $\beta = 0$ is plotted in grey (dark grey), $\beta = 0.001$ in blue (dark), and $\beta = 0.002$ in red (light grey).

FIG. 4 (color online). Time-frequency analysis obtained from the full integration of the 3D-TDSE and superimposed, in brown (dark), classical rescattering energies for the case of $\beta = 0.002$ and a plasmonic enhanced intensity of $I = 1.4 \times 10^{15}$ W/cm^2 corresponding to the case of Fig. 2.

independent of β and get noticeably different only for really high values of β. Similar behavior can be found in Fig. 3 for ionization times of $2.5 < t_i < 3.5$.

This effect has important consequences in the harmonic spectrum. The one plotted in Fig. 1 exhibits a wide zone where no clear harmonic peaks are visible, resulting in a continuum. As demonstrated in Ref. [23], a continuum obtained around 90 eV, using a 800 nm laser field using a single few-cycle pulse and homogeneous field, is a necessary condition for the generation of an isolated attosecond pulse. So far no clear method has been proposed to allow the generation of an isolated attosecond pulse in the keV region. Therefore, generating harmonics using the combined effect of temporal and spatial synthesis is a completely new route toward the generation of isolated attosecond pulses beyond the carbon K edge.

As a final test to confirm the underlying physics highlighted by the classical trajectories analysis, we retrieved the time-frequency distribution of the calculated dipole (from the 3D-TDSE) corresponding to the case of a nonhomogeneous laser field using a wavelet analysis. The result is presented in Fig. 4 where we have superimposed the calculated classical rescattering energies, in brown (dark), to show how the two calculations match. Analogously, in Fig. 4 we show the time-frequency analysis for the case of $\beta = 0.002$, which corresponds to the spectra presented in Fig. 1. The consistency of the classical calculations with the full quantum approach is clear and confirms that the mechanism of the generation of this $12.5U_p$ cutoff extension exhibiting a nice continuum is the consequence of trajectory selection and of the temporal lens effect on the recollision time, consequences of employing the combination of temporally and spatially synthesized laser field.

In conclusion, using laser fields constructed from a temporal superposition of two identical few-cycle pulses delayed in time together with a weak spatial non-homogeneity, we demonstrate that temporally and spatially synthesized laser fields are a new route for high harmonic generation, attosecond pulse production. We demonstrate that the main effect of this synthesized laser field on the harmonic generation is a considerable extension of the cutoff energy up to $12.5U_p$, which shows a large spectral continuum compatible with the generation of an isolated attosecond pulse beyond the carbon K edge. This effect is understood by analyzing the trajectories involved in the process using classical and fully quantum approaches. Both analyses converge on the same conclusion: trajectories are highly selected while using a laser field that consists of a combination of the double-pulse temporal synthesis and the spatial non-homogeneity. In addition, a "temporal lens effect" shrinks the recombination time window, resulting in a nice continuum generation in the extended harmonics spectral region. This new approach provides a unique route to the production of a coherent attosecond light source at energies beyond the carbon K edge directly from an 800 nm laser system and therefore is of interest for strong field applications in time-resolved x-ray spectroscopy of molecular systems.
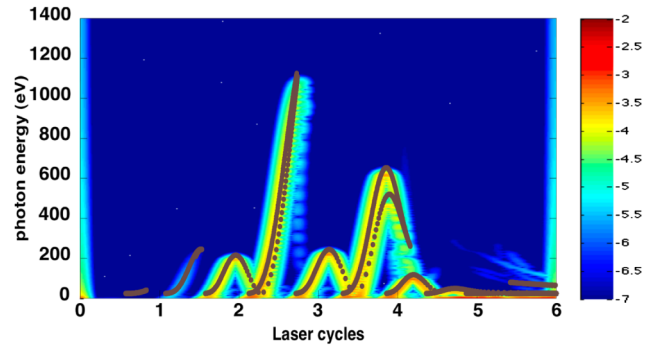
*joseap@usal.es

[1] J. J. Rehr and R. C. Albers, Rev. Mod. Phys. **72**, 621 (2000).
[2] C. Bressler and M. Chergui, Chem. Rev. **104**, 1781 (2004).
[3] S. Baker, J. S. Robinson, C. A. Haworth, H. Teng, R. A. Smith, C. C. Chirilă, M. Lein, J. W. G. Tisch, and J. P. Marangos, Science **312**, 424 (2006).
[4] A. Zaïr et al., Chem. Phys. (in press).
[5] M. Lewenstein, P. Balcou, M. Y. Ivanov, A. L'Huillier, and P. B. Corkum, Phys. Rev. A **49**, 2117 (1994).
[6] T. Popmintchev et al., Science **336**, 1287 (2012).
[7] J. Tate, T. Auguste, H. Muller, P. Salières, P. Agostini, and L. DiMauro, Phys. Rev. Lett. **98**, 013901 (2007).
[8] M. V. Frolov, N. L. Manakov, and A. F. Starace, Phys. Rev. Lett. **100**, 173001 (2008).
[9] J. A. Pérez-Hernández, L. Roso, and L. Plaja, Opt. Express **17**, 9891 (2009).
[10] Z. Zeng, Y. Cheng, X. Song, R. Li, and Z. Xu, Phys. Rev. Lett. **98**, 203901 (2007).
[11] E. J. Takahashi, T. Kanai, K. L. Ishikawa, Y. Nabekawa, and K. Midorikawa, Phys. Rev. Lett. **101**, 253901 (2008).
[12] C. Winterfeldt, C. Spielmann, and G. Gerber, Rev. Mod. Phys. **80**, 117 (2008).
[13] L. E. Chipperfield, J. S. Robinson, J. W. G. Tisch, and J. P. Marangos, Phys. Rev. Lett. **102**, 063003 (2009).
[14] L. E. Chipperfield, J. W. Tisch, and J. P. Marangos, J. Mod. Opt. **57**, 992 (2010).
[15] T. Siegel et al., Opt. Express **18**, 6853 (2010).
[16] L. Brugnera et al., Opt. Lett. **35**, 3994 (2010).
[17] G. Orlando, P. P. Corso, and E. Fiordilino, J. Mod. Opt. **57**, 2069 (2010).
[18] L. Brugnera, D. Hoffmann, T. Siegel, F. Frank, A. Zaïr, J. Tisch, and J. Marangos, Phys. Rev. Lett. **107**, 153902 (2011).
[19] R. A. Ganeev, V. V. Strelkov, C. Hutchison, A. Zaïr, D. Kilbane, M. A. Khokhlova, and J. P. Marangos, Phys. Rev. A **85**, 023832 (2012).
[20] K. Yuan and A. D Bandrauk, J. Phys. B **45**, 074001 (2012).
[21] J. J. Carrera, X. M. Tong, and S.-I. Chu, Phys. Rev. A **74**, 023404 (2006).
[22] J. A. Pérez-Hernández, D. J. Hoffmann, A. Zaïr, L. E. Chipperfield, L. Plaja, C. Ruiz, J. P. Marangos, and L. Roso, J. Phys. B **42**, 134004 (2009).
[23] G. Sansone et al., Science **314**, 443 (2006).
[24] P. Eckle, M. Smolarski, P. Schlup, J. Biegert, A. Staudte, M. Schöffler, H. G. Muller, R. Dörner, and U. Keller, Nat. Phys. **4**, 565 (2008).
[25] A. Husakou, S.-J. Im, and J. Herrmann, Phys. Rev. A **83**, 043839 (2011).
[26] I. Yavuz, E. A. Bleda, Z. Altun, and T. Topcu, Phys. Rev. A **85**, 013416 (2012).
[27] M. F. Ciappina, J. Biegert, R. Quidant, and M. Lewenstein, Phys. Rev. A **85**, 033828 (2012).
[28] M. Protopapas, C. H. Keitel, and P. L. Knight, Rep. Prog. Phys. **60**, 389 (1997).
[29] T. Brabec and F. Krausz, Rev. Mod. Phys. **72**, 545 (2000).
[30] V. Strelkov, E. Mevel and E. Constant, Eur. Phys. J. Special Topics **175**, 15 (2009).
[31] S. Kim, J. Jin, J. Jin, Y.-J. Kim, I.-Y. Park, Y. Kim, and S.-W. Kim, Nature (London) **453**, 757 (2008).
[32] I.-Y. Park, S. Kim, J. Choi, D.-H. Lee, Y.-J. Kim, M. F. Kling, M. I. Stockman, and S.-W. Kim, Nat. Photonics **5**, 677 (2011).
[33] S. Zherebtsov et al., Nat. Phys. **7**, 656 (2011).
[34] F. Süßmann and M. F. Kling, Proc. SPIE Int. Soc. Opt. Eng. **8096**, 80961C (2011).
[35] F. Süßmann and M. F. Kling, Phys. Rev. B **84**, 121406(R) (2011).
[36] P. Hommelhoff, Y. Sortais, A. Aghajani-Talesh, and M. A. Kasevich, Phys. Rev. Lett. **96**, 077401 (2006).
[37] M. Schenk, M. Krüger, and P. Hommelhoff, Phys. Rev. Lett. **105**, 257601 (2010).
[38] M. Krueger, M. Schenk, and P. Hommelhoff, Nature (London) **475**, 78 (2011).
[39] M. Krueger, M. Schen, M. Förster, and P. Hommelhoff, J. Phys. B **45**, 074006 (2012).
[40] G. Herink, D. R. Solli, M. Guld, and C. Ropers, Nature (London) **483**, 190 (2012).
[41] M. F. Ciappina, S. S. Aćimović, T. Shaaran, J. Biegert, R. Quidan, and M. Lewenstein, Opt. Express **20**, 26 261 (2012).
[42] X. M. Tong and C. D. Lin, J. Phys. B **38**, 2593 (2005).
[43] J. Feist, M. T. Homer Reid, and M. F. Kling, arXiv:1208.5905.
[44] K. Schafer, B. Yang, L. F. DiMauro, and K. C. Kulander, Phys. Rev. Lett. **70**, 1599 (1993).
[45] P. B. Corkum, Phys. Rev. Lett. **71**, 1994 (1993).
[46] A. Zaïr et al., Phys. Rev. Lett. **100**, 143902 (2008).